PACE: Predicting Adverse Cardiac Events in Breast Cancer Patients

Danielle Berera, Vasanth Sathiyakumar MS, Douglas Sawyer MD PhD, Lenneman MD MSCI

ABSTRACT

Background:
Breast cancer (BCA) affects one in eight women in the US. Doxorubicin (Dox) and Trastuzumab (Tsz) remain prevalent chemotherapies for breast cancer, but cause cardiotoxicty with significant morbidity and mortality in a subset of patients. The current study is a sub-study of an ongoing prospective observational study investigating if specific cardiac factors, growth factors, genetic polymorphisms and self-reported physical activity can predict which women will develop cardiac dysfunction from chemotherapy. The sub-study of PACE was aimed at characterizing the self-reported physical activity during first three months of chemotherapy.

Methods:
In a prospective, longitudinal study, 132 newly diagnosed breast cancer women receiving either AC or Tsz were enrolled over a 4-year period. Baseline data on age, BMI, personal history of hypertension, hyperlipidemia, diabetes mellitus, tobacco use, and coronary artery disease, family history of cardiomyopathy and self-reported physical activity at enrollment and at 4 time-points during first three-months of chemotherapy were ascertained. Enrolled participants were given baseline physical activity questionnaire and 4 additional CHAMPS questionnaire during chemotherapy (validated International Physical Activity Questionnaire – IPAQ and CHAMPS questionnaire respectively). CHAMPS questionnaire reported the various forms of physical activity in metabolic equivalent for task per hour per week (MET-hrs/wk). Complete questionnaires from 86 patients were analyzed.

Results:
The mean age of this cohort was 50 years old with a Caucasian predominance. Women average stage of breast cancer was Stage II. Physical activity significantly decreased in during Dox treatment in compared to TSZ. However looking at the combined group of Dox and TSZ there were a statically significant trend showing a overall decrease in self-reported physical activity.

Conclusions
Women enrolled in PACE have a high number of cardiovascular risk factors (hypertension, hyperlipidemia, and overweight). Our study demonstrates that most women describe a decrease in their physical activity during chemotherapy. It remains unknown if an exercise prescription decreases the likelihood of developing cardiotoxicity. Further work is needed with ongoing prospective studies.
.

INTRODUCTION

Adequate exercise for patients undergoing chemotherapy for cancer treatment is critical. Many studies have revealed that patients undergoing cancer treatment who exercise more than their counterparts report decreases in depression and fatigue with concurrent increases in muscle strength, aerobic capacity, mental health, and overall immune function[1-9]. Some longitudinal studies have also found overall decreases in long-term mortality rates in patients who exercise during chemotherapy[10-12]. The long-term benefits of exercise on the cardiovascular system have been well documented and include prevention of systolic and diastolic dysfunction and mitigation of elevated blood pressures[13]. The purpose of this study was to characterize the natural trend of self-reported physical activity during breast cancer treatment.

METHODS

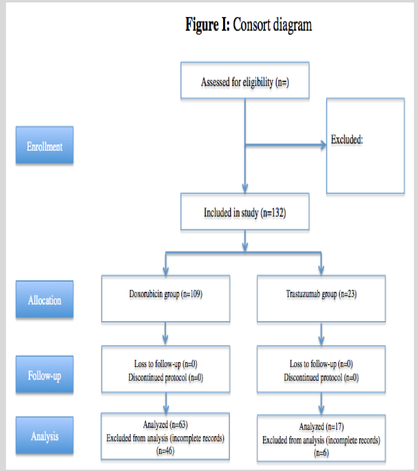

Fig. 1: Flow diagram for patient enrollment

METHODS – QUESTIONNAIRE SCHEME

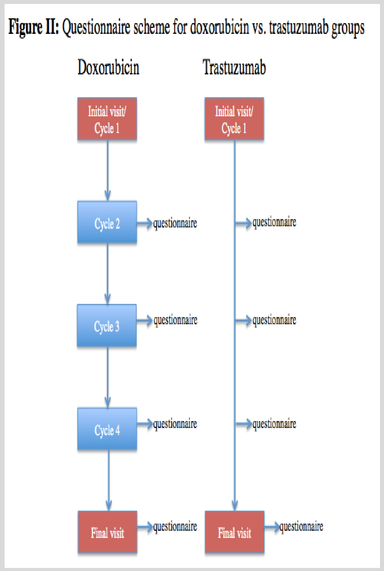

Fig. 2: IPAC and CHAMPS Questionaires were given at these corresponding times.

RESULTS – PATIENT CHARACTERISTICS

Table I: Baseline demographics and cancer characteristics

	Trastuzumab	Doxorubicin	p-value
Average age			
Gender			
Female	17 (100.0%)	63 (100.0%)	0.999
Male	0 (0.0%)	0 (0.0%	
Race			
Caucasian	16 (94.1%)	54 (85.7%)	0.801
African-American	1 (5.9%)	7 (11.1%)	
Other	0 (0.0%)	2 (3.2%)	
Cancer stage			
Stage I	8 (47.1%)	7 (11.1%)	0.006
Stage II	4 (23.5%)	37 (58.7%)	
Stage III	4 (23.5%)	14 (22.2%)	
Unknown	1 (5.9%)	5 (7.9%)	
Tumor stage			
T1	10 (58.8%)	22 (34.9%)	0.1
T2	2 (3.2%)	25 (39.7%)	
T3	3 (4.8%)	8 (12.7%)	
T4	1 (5.9%)	1 (1.6%)	
Unknown	1 (5.9%)	7 (11.1%)	
Nodal stage			
N0	9 (52.9%)	18 (28.6%)	0.455
N1	6 (35.3%)	33 (52.4%)	
N2	1 (5.9%)	6 (9.5%)	
N3	0 (0.0%)	2 (3.2%)	
Unknown	1 (5.9%)	4 (6.3%)	
Metastatic stage			
M0	16 (94.1%)	55 (87.3%)	0.676
Unknown	1 (5.9%)	8 (12.7%)	

Table II: Baseline medical and medication history

	Trastuzumab	Doxorubicin	p-value
Medical history			
Hx hypertension	6 (35.3%)	20 (31.7%)	0.778
Hx ventricular dilation	0 (0.0%)	0 (0.0%)	0.999
Hx systolic dysfunction	0 (0.0%)	0 (0.0%)	0.999
Hx heart failure	0 (0.0%)	0 (0.0%)	0.999
Hx hyperlipidemia	2 (3.2%)	18 (28.6%)	0.214
Hx coronary artery disease	0 (0.0%)	0 (0.0%)	0.999
Hx arrhythmia	1 (5.9%)	7 (11.1%)	0.999
Hx diabetes	1 (5.9%)	4 (6.3%)	0.999
Hx family cardiomyopathy	2 (11.8%)	21 (33.3%)	0.130
Medication history			
Beta-blocker	1 (5.9%)	11 (17.5%)	0.444
ACE-I/ARB	3 (17.6%)	9 (14.3%)	0.711
Diuretic	1 (5.9%)	10 (15.9%)	0.441
Aspirin	0 (0.0%)	2 (3.2%)	0.999
Substance history			
Tobacco			
Never	14 (82.4%)	45 (71.4%)	0.577
Ex-smoker	2 (11.8%)	16 (25.4%)	
<1 PPD	0 (0.0%)	1 (1.6%)	
>1 PPD	0 (0.0%)	1 (1.6%)	
Alcohol			
None	8 (47.1%)	22 (24.9%)	0.467
<1 per day	7 (41.2%)	38 (60.3%)	
1-2 per day	1 (5.9%)	2 (3.2%)	
3-5 per day	0 (0.0%)	1 (1.6%)	

RESULTS – CHANGE IN EXERCISE

Figure III: Average MET-h/week based on treatment protocol

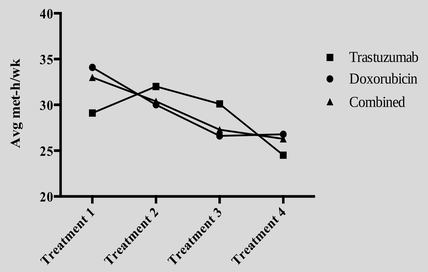

	T1	T2	T3	T4	p-value
Doxorubicin	34.1	30.0	26.6	26.8	0.014
Trastuzumab	39.1	32.0	30.1	24.5	0.578
Combined	33.0	30.4	27.3	26.3	0.044

RESULTS – CHANGE IN WEIGHT

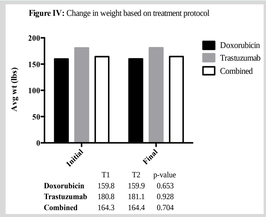

	T1	T2	p-value
Doxorubicin	159.8	159.9	0.653
Trastuzumab	180.8	181.1	0.928
Combined	164.3	164.4	0.704

Figure IV illustrates the average weights of patients at the initial study visit and the final study visit (~12 weeks after the initial visit). For all patients in the study, there was almost no change in the average weight from start to end of the study (p=0.704). This trend was also seen in sub-group analyses for patients in the doxorubicin and trastuzumab groups (p=.653 and p=.928 respectively).

CONCLUSION

- Women enrolled in PACE have a high number of cardiovascular risk factors (hypertension, hyperlipidemia, and overweight).
- Our study demonstrates that most women describe a decrease in their physical activity during chemotherapy.
- It remains unknown if an exercise prescription decreases the likelihood of developing cardiotoxicity.
- Further work is needed with ongoing prospective studies to investigate the effect of exercise on cardiac function during chemotherapy treatment.

ACKNOWLEDGEMENTS

- This project was supported in part by Lisa M. Jacobson Chair in Cardiovascular Medicine, Nashville, TN, USA (DBS), HL068144, Heart Failure Society of America Research Fellowship Grant, Saint Paul, Minnesota, USA (CGL), and Vanderbilt CTSA grant 1 UL1 RR024975 from NCRR/NIH, Nashville, TN, USA (CGL).
- We want to acknowledge and thank all the women who participated in this voluntary study.
- Research supported by grant R25-CA-134283 from the National Cancer Institute

REFERENCES

1. Carayol M, Bernard P, Bolche J et al. Psychological effect of exercise in women with breast cancer receiving adjuvant therapy: what is the optimal dose needed? Ann Oncol. 2013 Feb; 24(2): 291-300.
2. Badger T, Segrin C, Dorros SM et al. Depression and anxiety in women with breast cancer and their partners.
3. Battaglini CL, Mihalik JP, Bottaro M et al. Effect of exercise on the caloric intake of breast cancer patients undergoing treatment. Braz J Med Biol Res. 2008 Aug; 41(8):709-15.
4. Campbell A, Mutrie N, White F et al. A pilot study of a supervised group exercise programme as a rehabilitation treatment for women with breast cancer receiving adjuvant treatment. Eur J Oncol Nurs. 2005 Mar; 9(1):56-63.
5. Haines TP, Sinnamon P, Wetzig NG. Multimodal exercise improves quality of life of women being treated for breast cancer, but at what cost? Randomized trial with economic evaluation. Breast Cancer Res Treat. 2010 Nov; 124(1):163-75.
6. Hwang JH, Chang HJ et al. Effects of supervised exercise therapy in patients receiving radiotherapy for breast cancer.
7. Mock V, Dow KH, Meares CJ et al. Effects of exercise on fatigue, physical functioning, and emotional distress during radiation therapy for breast cancer. Oncol Nurs Forum. 1997 Jul; 24(6):991-1000.
8. Mock V, Frangakis C, Davidson NE et al. Exercise manages fatigue during breast cancer treatment: a randomized controlled trial.
9. Raghavendra RM, Nagarathna R, Nagendra HR et al. Effects of an integrated yoga programme on chemotherapy-induced nausea and emesis in breast cancer patients. Eur J Cancer Care. 2007 Nov; 16(6):462-74.
10. Holick CN, Newcomb PA, Trentham-Dietz A et al. Physical activity and survivial after diagnosis of invasive breast cancer. Cancer Epidemiol Biomarkers Prev. 2008 Feb; 17(2):379
11. Irwin ML, Smith AW, McTiernan A et al. Influence of pre- and postdiagnosis physical activity on mortality in breast cancer survivors: the health, eating, activity, and lifestyle study J Clin Oncol. 2008 Aug; 26(24):3958-64.
12. Sternfeld B, Weltzien E, Quesenberry CP Jr et al. Physical activity and risk of recurrence and mortality in breast cancer survivors: findings from the LACE study. Cancer Epidemiol Biomarkers Prev. 2009 Jan; 18(1):87-95.
13. Myers J. Exercise and cardiovascular health. Circulation. 2003; 107:e2-5.
14. Patterson RE, Cadmus LA, Emond JA et al. Physical activity, diet, adiposity, and female breast cancer prognosis: A review of the epidemiologic literature. Matr. 2010 May; 66(1):5-15.
15. Yang CY, Tsai JC, Huang YC et al. Effects of a home-based walking program on perceived symptom and mood status in postoperative breast cancer women receiving adjuvant chemotherapy. J Adv Nurs. 2011 Jan; 67(1):158-68.
16. Scott E, Daley AJ, Doll H et al. Effects of an exercise and hypocaloric healthy eating program on biomarkers associated with long-term prognosis after early-stage breast cancer: a randomized controlled trial. Cancer Causes Control. 2013 Jan; 24(1):181-91

Calorimetry of the Plasma Proteome in Patients with Ovarian Cancer

Mary Hatch[2], Alagammai Kaliappan[1,2], Nick Allen[3], Nichola Garbett[1,2]

James Graham Brown Cancer Center[1]

University of Louisville School of Medicine[2]

University of Louisville School of Engineering[3]

Introduction

- Ovarian cancer has a 65% mortality rate due to lack of early screening and diagnostic technologies.1
- Ovarian cancer symptoms are non-specific—bloating, dysphagia, change in bowel movements, general discomfort.
- Current diagnostic approaches are MRI, CT, PET, CA-125 levels, and highly invasive biopsy.
- Calorimetry has proven a useful non-invasive screening tool in Lyme Disease, Lupus, Rheumatoid Arthritis, and cervical cancer.2,3
- Calorimetry is performed using a differential scanning calorimeter (DSC), which compares the difference in excess specific heat capacity between sample and reference solutions as a function of temperature—this plot is referred to as a "thermogram."
- Plasma samples from five women with stage IIIC, epithelial ovarian cancers, with various levels of CA-125 were chosen for this study. The ovarian cancer of patient OC6 was of mesenchymal origin.
- One pooled healthy plasma control and one case-specific plasma control (OC5) were used for reference.
- The techniques used to examine the plasma samples were HPLC-SEC, BCA assay, SDS gel electrophoresis, and DSC.
- The goal of this project was to observe thermogram changes between healthy and diseased plasma samples and further investigate these alterations using HPLC-SEC, DSC, and mass spectrometry.

Methods

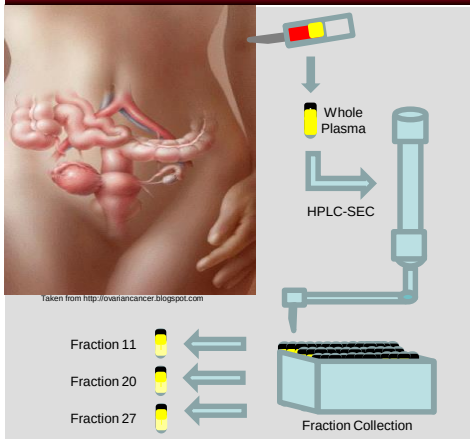

References

[1]"What Are the Key Statistics about Ovarian Cancer?" *Cancer.org*. 11 Aug. 2014. Web. 10 Sept. 2014.

[2]Garbett, Nichola C., James J. Miller, Alfred B. Jenson, and Jonathan B. Chaires. "Calorimetry Outside the Box: A New Window into the Plasma Proteome." *Biophysical Journal* (2007): 1377-383. Web. 10 Sept. 2014. <http://www.ncbi.nlm.nih.gov/pmc/articles/PMC2212685/>.

[3]Garbett, Nichola C., Michael L. Merchant, C. William Helm, Alfred B. Jenson, Jon B. Klein, Jonathan B. Chaires, and Jose M. Sanchez-Ruiz. "Detection of Cervical Cancer Biomarker Patterns in Blood Plasma and Urine by Differential Scanning Calorimetry and Mass Spectrometry." *PLoS ONE* (2014): E84710. Print.

"TUMOR IMMUNOLOGY." *TUMOR IMMUNOLOGY*. Web. 10 Sept. 2014. <http://pathmicro.med.sc.edu/mobile/m.immuno-18.htm>.

Thermograms of Individual Proteins in Plasma

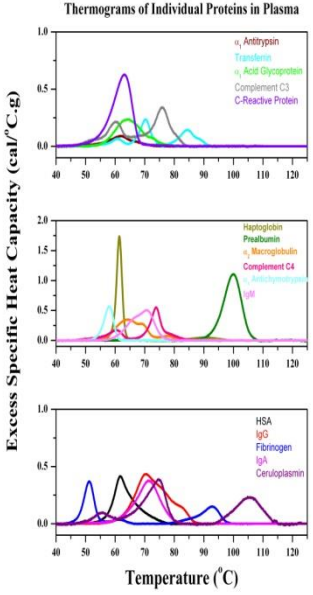

Pure Protein and Ovarian Cancer Elution Profiles

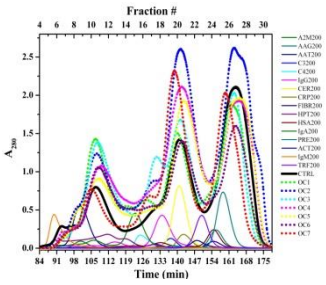

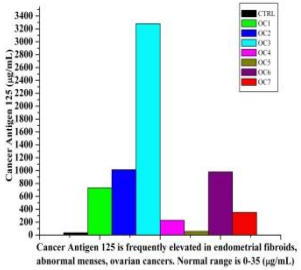

DSC Thermograms of Whole Plasma

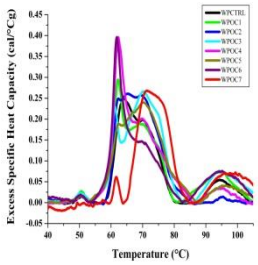

SDS Gel Electrophoresis of Whole Plasma

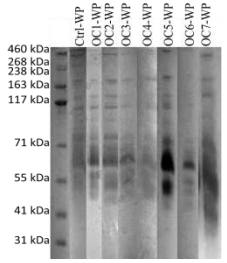

DSC Thermograms of Fraction 11

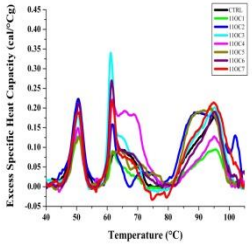

SDS Gel Electrophoresis of Fraction 11

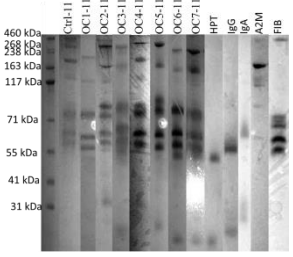

DSC Thermograms of Fraction 20

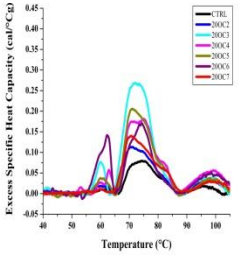

SDS Gel Electrophoresis of Fraction 20

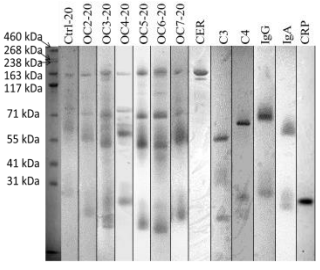

DSC Thermograms of Fraction 27

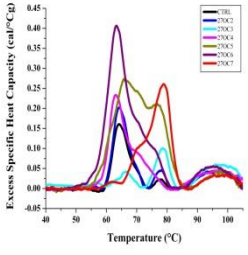

SDS Gel Electrophoresis of Fraction 27

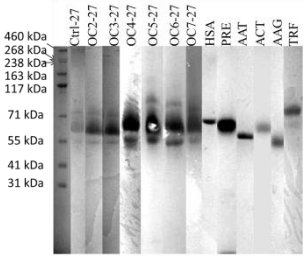

Results and Discussion

- Whole Plasma: The thermograms of OC2, OC3, OC5, and OC7 were significantly different from the healthy control. These gross changes are attributed to changes in concentration and interaction of abundant plasma proteins; primarily haptoglobin (HPT), albumin (HSA), and immunoglobulins (Ig). Enrichment of altered plasma fractions were pursued through HPLC-SEC.
- HPLC-SEC Chromatography: Deviations in shape are likely representative of differences in protein interactions or content.
- Based on these deviations, fractions 8-12, 17-22, and 25-28 were selected for DSC analysis.
- Fraction 11: Increased excess specific heat capacity at 62.5°C infers increased HPT concentration. The thermogram changes between 65°C and 70°C are indicative of changes in denaturation profiles of fibrinogen (FIB), Ig and alpha-2-macroglobulin (A2M).
- Fraction 20: Peak variation between 55°C and 65°C may be caused by ceruloplasmin (CER), complement proteins (C3,C4), and C-reactive protein (CRP). Significant peak variation between 65°C and 85°C are indicative of changes in CER, C3/C4, and Ig.
- Fraction 27: Substantial shifts were observed in OC3, OC5, and OC7. This fraction is dominated by HSA; the thermogram differences suggest changes in HSA levels and protein interactions. Changes in prealbumin (PRE), transferrin (TRF), alpha-1-antichymotrypsin (ACT), alpha-1-acid glycoprotein (AAG), and alpha-1-antitrypsin (AAT) could also be contributory.
- The major alterations to the whole plasma thermograms are consequently described by changes in HSA, HPT, Ig, C3/C4, CER, and A2M. Other key players include FIB, TRF, CRP, PRE, AAT, ACT, AAG. Both protein levels and interactions may contribute to the observed changes.

Conclusions

- DSC is a non-invasive technique that can screen for disease in blood plasma.
- HPLC-SEC allows identification of proteins causing shifts in the whole plasma thermograms.
- Changes in thermal profiles of these proteins infer alterations to the abundant proteome in ovarian cancer. These changes could result from alterations in protein interactions in the presence of tumor specific antigens or from post-translational modifications to abundant plasma proteins.

Future Work

- Increase the number of samples for statistical significance.
- Mass spectrometry will be applied to identify the presence of disease-specific markers and to investigate the nature of changes in the ovarian cancer proteome.
- Explore the differences in plasma proteomes between ovarian cancers of varying origins (epithelial, germ cell, stromal, etc.)

Acknowledgements

This work was supported by:

- National Cancer Institute grant R25-CA134283
- Competitive matching grant, University of Louisville School of Medicine
- James Graham Brown Cancer Center

Inhibition of melanoma metastases by targeting regulator of G protein signaling 2 (RGS2)

Deepa Patel, M.S.[1], Deyi Xiao, M.D. [1], Hongying Hao, M.D., Ph.D.[1], Kelly M. McMasters, M. D., Ph. D.[1]
Department of Surgery[1], University of Louisville School of Medicine

Abstract

While new targeted therapies for melanoma have been developed recently, the prognosis for metastatic melanoma remains dismal. To that end, the investigation of mechanisms for melanoma progression is an important translation research area that can bridge basic science with clinical practice. In cutaneous melanoma, the mitogen activated protein kinase (MAPK) is constitutively activated. Activation of this pathway leads to the induction of epithelial-to–mesenchymal transition (EMT), a process that resembles the genesis of cancer stem-like cells resulting in tumor invasion, aggressiveness, and metastasis. The regulator of G protein signaling (RGS) protein plays an important role in the development of vasculature. RGS family members are regulatory molecules that act as GTPase activating proteins (GAPs) for G alpha subunits of heterotrimeric G proteins. However, none of the current research has entailed the connection of RGS with melanoma progression. This project used an established melanoma progression model to show that one of the RGS family members, RGS2, was upregulated in highly metastatic melanoma cell lines. Upregulation of RGS2 in metastatic cell lines was also associated with hyperactivated MAPK pathway and induction of EMT. Manipulated expression of RGS caused increased migration and invasion abilities in less-metastatic melanoma cells by RGS2 plasmid transfection or decreased metastatic potential by RGS2 siRNA knockdown in highly-metastatic melanoma cells. These results confirm that over expression of RGS2 can promote melanoma metastasis by inducing EMT through activation of the MAPK pathway. It provides a starting point for mechanism-based evidence in support of RGS2 as a therapeutic target for inhibiting melanoma progression.

Introduction

- **RGS2 is a GTPase regulatory protein that is overexpressed in aggressive metastatic melanoma cell lines**
- **Epithelial-mesenchymal transition (EMT) is a molecular program whereby epithelial cells undergo reprogramming so that they are now able to migrate into vasculature and lymph thus initiating metastatic progression. EMT is activated through the MAPK pathway.**
- **Analyzing the role of RGS in promoting melanoma progression through EMT could lead to new therapeutic targets**

Methods

An A375 established melanoma progression model was used with three generations having increasing metastatic potential (A375P, A375MA1, A375MA2):

1)RGS2, EMT markers, and MAPK expression were checked using Real-time PCR and Western Blot.

2)Migration abilities of (A375MA2/A375MA1 vs A375P) were checked using an assay

3)RGS2 was knocked down using siRNA transfection. Migration and invasion assays were conducted to determine metastatic potential. RGS2 levels were confirmed using Real- time PCR and Western Blot.

4)RGS2 was upregulated using plasmid transfection. Migration and invasion assays were conducted to determine metastatic potential. RGS2 levels were confirmed using Real-time PCR and Western Blot.

Results

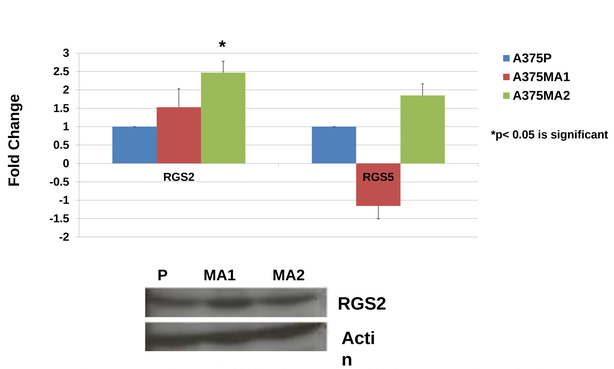

Figure 1. Upregulation of RGS: Real-Time PCR and Western Blot results

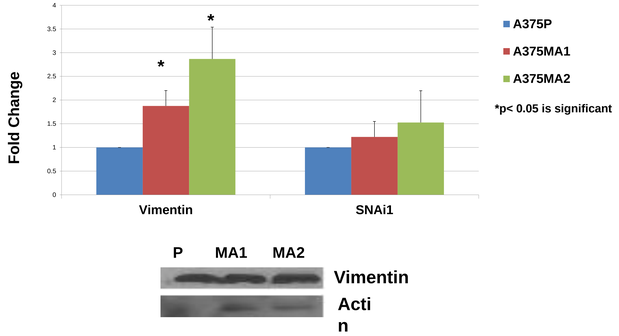

Figure 2. Upregulation of EMT Markers: Real-Time PCR and Western Blot results

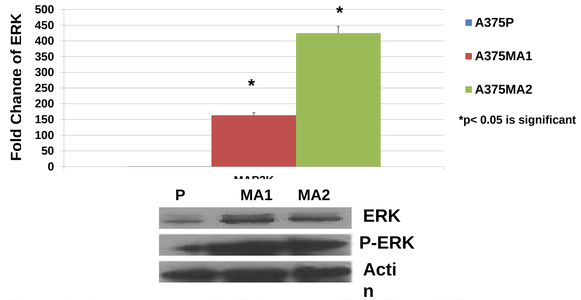

Figure 3. Upregulation of MAPK Kinases: Real-Time PCR and Western Blot results

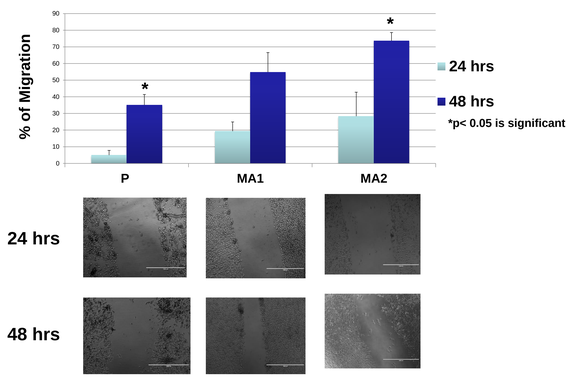

Figure 4. Migration Assay A375 MA2/ MA1 vs. A375P

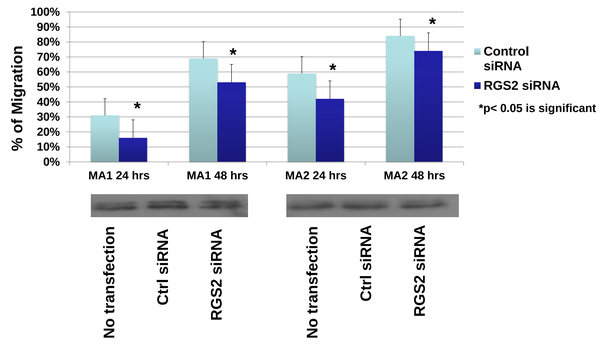

Figure 5. Migration assay after RGS2 siRNA transfection in A375MA1 and A375MA2

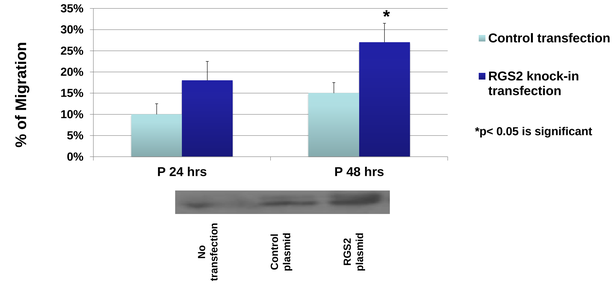

Figure 6. Migration assay after RGS2 plasmid transfection in A375P

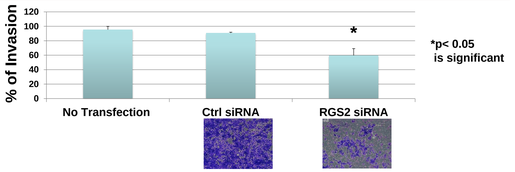

Figure 7. A375MA2 RGS2 siRNA transfection invasion assay

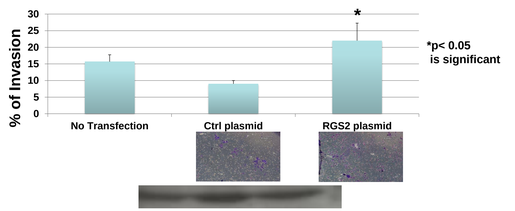

Figure 8. A375P RGS2 plasmid transfection invasion assay

Conclusions

- **RGS2, EMT markers, and MAPK are upregulated in highly metastatic cells lines (A375MA1/MA2) vs poorly metastatic cell line (A375P).**
- **RGS2 siRNA transfection knockdown cell lines showed decreased migration and invasion potential (MA1/MA2 vs P)**
- **RGS2 plasmid transfection knock-in cell lines showed increased migration and invasion potential (MA1/MA2 vs P)**
- **Overexpression of RGS2 promotes melanoma metastasis by inducing EMT through activation of MAPK**
- **These findings could lead to new therapeutic targets for inhibiting melanoma progression**

Acknowledgements

Research supported by NCI R25 grant University of Louisville Cancer Education Program NIH/NCI (R25-CA134283).We thank Dr. Richard Hynes for giving us the A375P cells and its metastatic variants.

UNIVERSITY OF LOUISVILLE
It's Happening Here.®

Isolating miRNAs and their mRNA Targets in Lung Adenocarcinoma Tumors *versus* Normal Adjacent Lung Tissue

David R. Patterson, Andrea Y. Angstadt, & Carolyn M. Klinge
Department of Biochemistry & Molecular Biology; Center for Genetics & Molecular Medicine
University of Louisville School of Medicine, Louisville, KY 40292

Abstract

MicroRNAs (miRNAs) act as oncomiRs, tumor suppressors, and as post-transcriptional regulators of target mRNAs by binding to sites in the mRNA 3'UTR in the RNA-induced silencing complex (RISC) containing Argonaute (Ago) proteins. Published expression studies of miRNA in lung cancer provide a global level of expression and may not be indicative of miRNA functionality, which is important for the identification of candidate therapeutic targets. This study hypothesized that miRNAs and mRNAs interact with one another in complex reaction networks that differentiate lung adenocarcinoma, a type of non-small cell lung cancer (NSCLC) that is increasing globally in men and women and in smokers and non-smokers, from normal adjacent lung tissue. A newly developed protocol, high-throughput sequencing together with UV-crosslinking and immunoprecipitation (HITS-CLIP), was performed on A549 cells and flash frozen lung adenocarcinomas and normal adjacent tissue. This study uniquely isolated miRNA-mRNA complexes by immunoprecipitation with the Ago2 protein using radiolabeled linkers to follow the complex during purification. Further RNA isolation was performed by protease digestion and phenol-chloroform extraction. Then, RT-PCR and subsequent gel extraction was utilized to amplify bound miRNA-mRNA complexes to which linkers were ligated and the tagged RNA has been sent to RNA sequencing. This study successfully isolated and prepared for sequencing stable miRNA-mRNA complexes bound to Ago2 in lung adenocarcinomas and normal adjacent tissues. Once the samples are sequenced, this study will enter the bioinformatics stage to identify the differentially expressed miRNA-mRNA complexes in lung adenocarcinoma versus normal adjacent tissue.

Background/Hypothesis

MicroRNA

Single-stranded, small RNAs that are involved in post-transcriptional downregulation of protein expression by binding to mRNAs and preventing translation into a protein and, in some cases, initiating mRNA degradation. Dysregulation of microRNAs (miRNAs) are thought to be a promoting factor of the oncogenic nature of cancer .

HITS-CLIP

High-throughput sequencing of RNA isolated by crosslinking immunoprecipitation (HITS-CLIP) UV radiation is used to cross -link protein-RNA complexes. Immunoprecipitation of the Argonaute:miRNA :mRNA complex, followed by subsequent RNA isolation and library preparation, yields a transcriptome-wide map of miRNA binding sites.

Hypothesis

Expression of miRNA:mRNA complexes is different between lung adenocarcinomas and adjacent normal lung tissue.

Material & Methods

- Human Lung Tumor and adjacent normal tissue were obtained from the UofL Biorepository (IBC #11-035(M1) to CMK 5/1/13)
- A549 human lung adenocarcinoma cells were obtained from ATCC
- Tissue crosslinked by UV irradiation – forms covalent crosslinks between Ago2 and mRNA. Excess UV irradiation was avoided to prevent damage to Ago2:RNA complexes.
- Dynabeads were prepared using monoclonal antibody 2A8, which recognizes the Ago2 protein.
- Cells were lysed with 1x PXL.
- mRNA was digested to about 40 nucleotides long using RNase A
- Samples were centrifuged and supernatant was collected
- Ago2-RNA complexes in the supernatant were bound to prepared dynabeads
- The 3' end of the RNA tags was dephosphorylated using alkaline phosphatase
- [^{32}P]-Labeled linker was added to the free 3' end of the RNA using T4 RNA ligase I
- The 5' end of the RNA tags were phosphoryalted using T4 PNK
- Ago2:RNA complexes were dissociated from dynabeads into solution using LDS sample buffer and run on a Novex NuPAGE Bis-Tris gel.
- The complexes were transferred to a nitrocellulose membrane
- The [^{32}P]-Labeled RNA tags were detected by audioradiography with Carestream BIOMAX MR film
- Extraction of RNA
- Addition of 5'linker and RT-PCR
- Addition of sequencing adaptors and PCR
- Gel extraction and purification for sequencing

Protocol based on Moore *et al*. Darnell Nature Protocols 9: 263-93, 2014

D.R.P. was supported by NCI R25-CA-134283. The research was supported by a Kentucky Lung Cancer Research Program grant to C.M.K.

Material & Methods

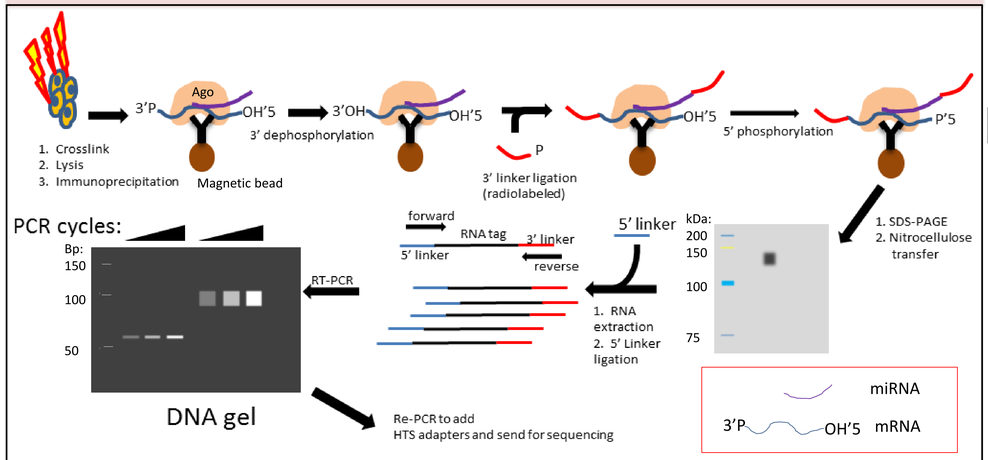

Figure 1. HITS-CLIP. Method used to identify miRNA targets bound to Ago:miRNA:mRNA complex by immunoprecipitation, radiolabeling, RT-PCR, and addition of sequence adaptors.

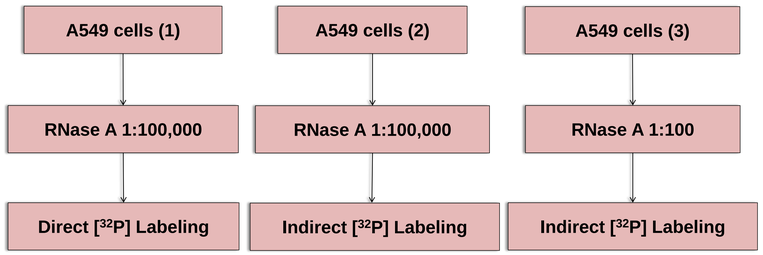

Figure 2. Schematic representation of the trial experimental procedure using the A549 lung adenocarcinoma cell line to perform HITS-CLIP.

Results

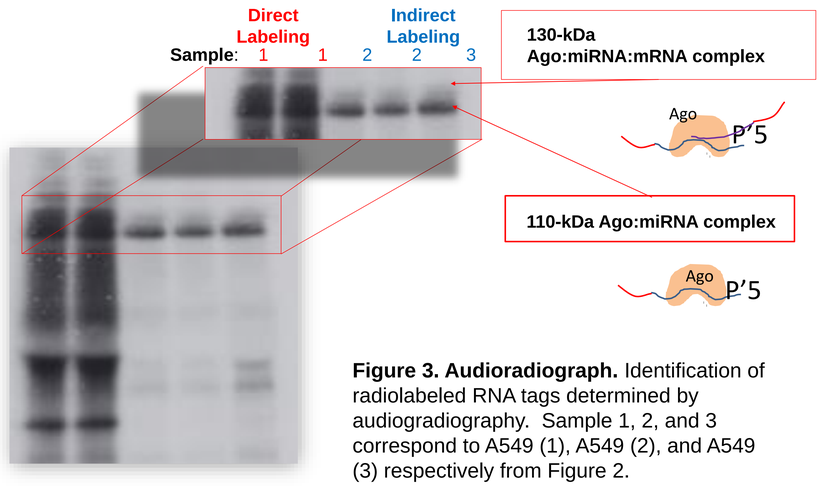

Figure 3. Audioradiograph. Identification of radiolabeled RNA tags determined by audiogradiography. Sample 1, 2, and 3 correspond to A549 (1), A549 (2), and A549 (3) respectively from Figure 2.

Results

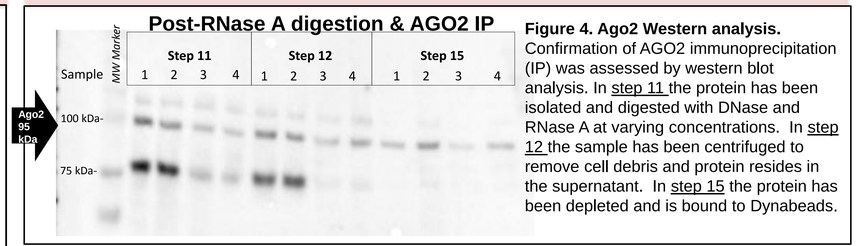

Figure 4. Ago2 Western analysis. Confirmation of AGO2 immunoprecipitation (IP) was assessed by western blot analysis. In step 11 the protein has been isolated and digested with DNase and RNase A at varying concentrations. In step 12 the sample has been centrifuged to remove cell debris and protein resides in the supernatant. In step 15 the protein has been depleted and is bound to Dynabeads.

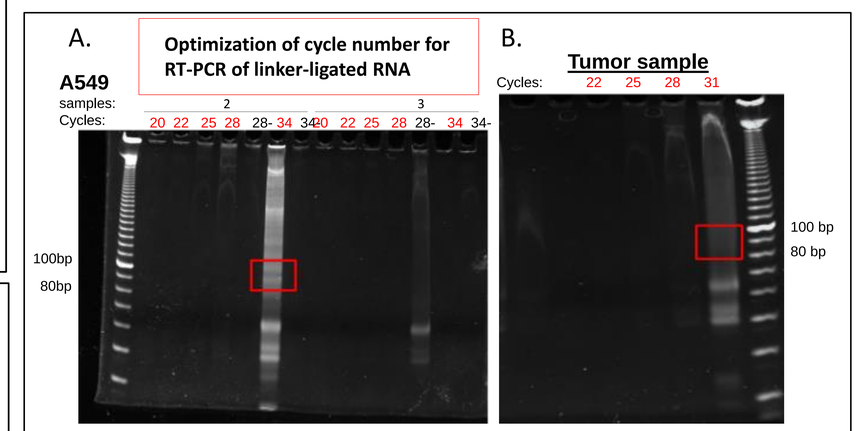

Figure 5. RT-PCR gel images of samples from A549 cells (A) and lung adenocarcinomas (B). The samples were excised from a nitrocellulose membrane according to protein size, RNA isolated, and a 5'linker was ligated to the RNA tags. The RNA tags were modified with adapter sequences and amplified by RT-PCR. Overamplification was avoided to decrease predominance of select RNA tags. DNA between 80 and 100 base pairs was excised (**red squares**) for gel extraction. "28-" and "34-" represent controls with no added reverse transcriptase.

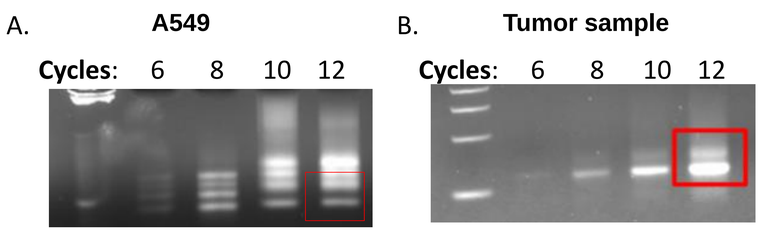

Figure 6. Addition of sequencing adaptors to gel extracted RT-PCR DNA fragments. A and B represent A549 cells and lung adenocarcinoma respectively. DNA between 147 and 177 base pairs was excised (**red squares**) for gel extraction, isolated and purified for future sequencing.

Conclusions

- **Stable miRNA-mRNA complexes were successfully isolated and prepared for RNA sequencing from flash frozen human lung adenocarcinoma tumors.**
- **Once the samples are sequenced, this study will enter the bioinformatics stage to identify specific miRNA-mRNA complexes differentially expressed in lung adenocarcinoma and normal adjacent tissue.**

Development of Theranostic Mesoporous Silica Nanoparticles for Pancreatic Cancer

Dillon S. Pender, Anil Khanal, Shanice V. Hudson, Lacey R. McNally

Department of Medicine, University of Louisville, Louisville, KY

ABSTRACT

Introduction: Modern methods of pancreatic cancer diagnosis and treatment are severely lacking and have failed to provide effectual treatment options for patients. The root cause of this inadequacy stems from the hypovascularized nature of pancreatic cancer, making traditional chemotherapeutics and cancer detecting contrast agents nearly obsolete. A potential solution for tumor-targeting difficulties is through the implementation of nanotechnology, specifically targeting ligand capped, theranostic nanoparticles. We hypothesize that pH-responsive chitosan-capped mesoporous silica nanoparticles (MSNs) with the targeting ligand, urokinase plasminogen activator (UPA) will serve as theranostic agents for treatment and diagnosis of pancreatic cancer.

Methods: MSNs were synthesized by employing cetyl trimethylammonium bromide (CTAB), tetraethyl orthosilicate (TEOS) and chitosan through the sol-gel method. The synthesized MSNs were characterized by transmission electron microscopy (TEM) and zeta-potential measurements. Afterwards, gemzar chemotherapeutic drug was encapsulated into these nanoparticles to observe the pH dependent release profiles *in-vitro*. Furthermore, MSNs were tagged with UPA to increase the binding efficiency of these nanoparticles towards the pancreatic tumor cells (S2CP9 and S2VP10). The binding efficiency of both tagged and non-tagged MSNs was observed at various pHs (7.4 to 6.5) by employing fluorescence microscopy, Odyssey infrared imaging and tissue phantoms. For that, various types of dyes were used, such as, rhodamine B and with indocyanine green (ICG). Finally, UPA-tagged MSNs with ICG were injected into mice infected with S2CP9 tumors cells to observe the distribution of these nanoparticles *in*-vivo by multispectral photoacoustic Tomography system (MSOT).

Results: TEM pictures showed that the synthesized MSN had a size around 120 nm. Zeta-potential measurements revealed that charge density of MSN dependent on pH. The release experiments showed that these nanoparticles were pH-sensitive because the release of gemazar depended on the pH. Gemzar released ~2x the quantity from MSNs at pH 6.5 in comparison to pH 7.4. Fluorescence microscopy, Odyssey infrared imaging and tissue phantoms showed that uptake of MSNs by pancreatic tumor cells depended on the pH and tagging of UPA. Lowering a pH and tagging a ligand drastically increased the uptake of MSNs in pancreatic tumor cell *in-vitro*. Specifically in tissue phantoms, UPA-ICG loaded MSNs at pH 6.5 demonstrated 20X and 7X more cell signal than without ligand or at pH 7.4, respectively. Furthermore, UPA-ICG loaded MSNs were successfully detected in orthotopic pancreatic tumor of mice within 4 hours of imaging time by MSOT.

Conclusion: UPA tagged, pH sensitive MSNs demonstrate potential as a theranostic nanoparticle for pancreatic cancer.

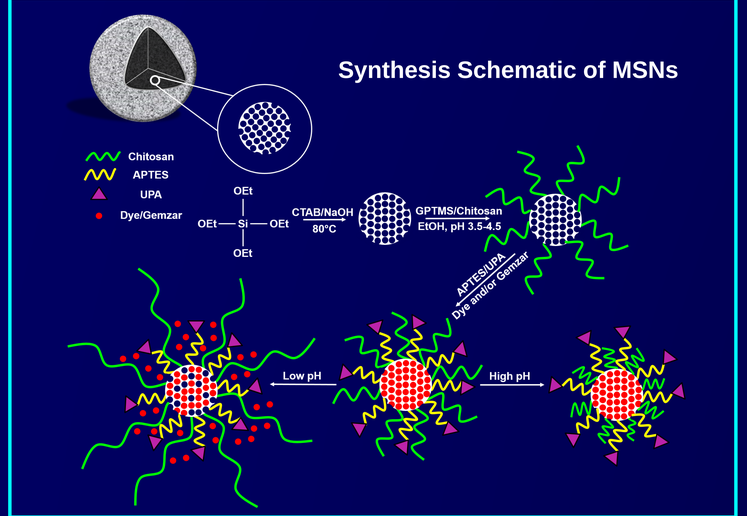

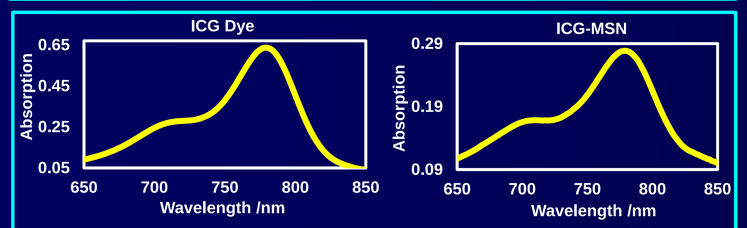

Figure 1: UV-Vis spectrum of indocyanin green (ICG) and ICG loaded MSNs. Graphs show same absorbance peak of ~780 nm. The consistency in absorbance between the two specimens indicates loading of the MSNs with the ICG dye and validates that the MSNs to possess fluorescent capabilities.

RESULTS

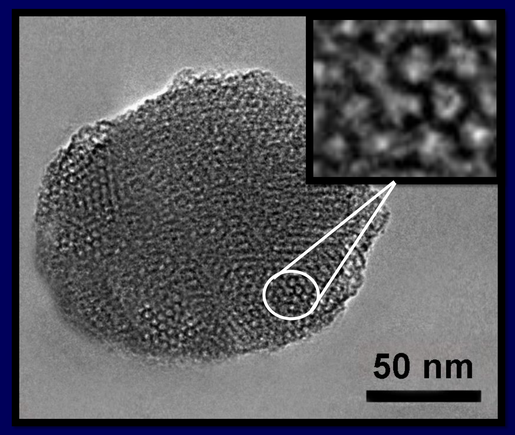

Figure 2: Transmission electron microscopy image of MSNs. After MSN particles were synthesized, particles were dried onto lacey-carbon coated grids and viewed. MSN particles contained visible mesoporous, spherical structures with a diameter of ~120 nm and a pore size of ~3 nm.

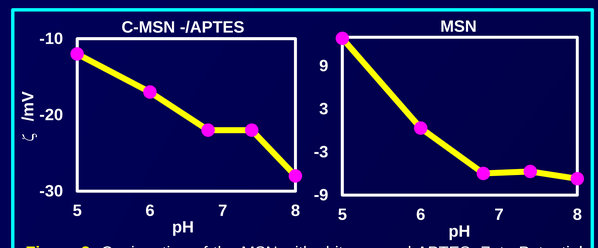

Figure 3: Conjugation of the MSN with chitosan and APTES. Zeta Potential analysis validates the conjugation of chitosan conjugated MSN, (C-MSN -/APTES) chitosan and (3-Aminopropyl) triethoxysilane (APTES) (not shown), dual conjugated MSN (MSN). The decreasing voltage with corresponding increases in pH results from lessened protonation of the chitosan compound. The addition of APTES adds positive charge to the particle resulting in a more positive charge for the C-MSN-AP when compared to the C-MSN.

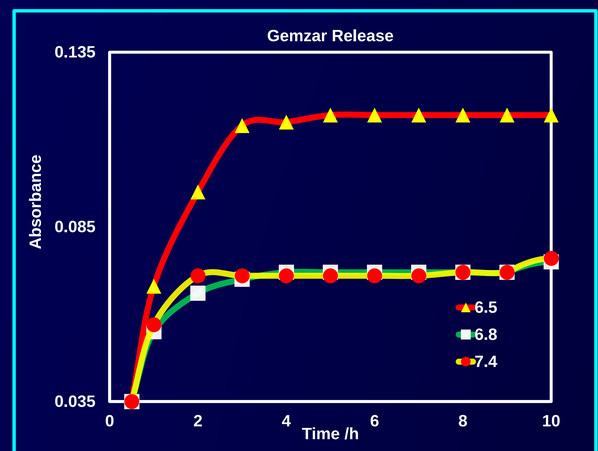

Figure 4: Gemzar-loaded MSNs were evaluated for pH specific drug release. The Gemzar-MSN solutions were incubated in phosphate buffer saline (PBS) solution of either 6.5, 6.8, or 7.4 pH. Release of Gemzar was based upon absorbance measured using UV-Vis spectroscopy over a period of 10 hours. The amount of absorbance found in PBS solution directly correlated to the level of Gemzar drug that had been released from the MSNs. The MSNs at pH 6.5 were found to release ~2x the amount of Gemzar as compared to the MSNs kept at pH 6.8 and 7.4. These results illustrate the effective pH sensitivity of the MSNs.

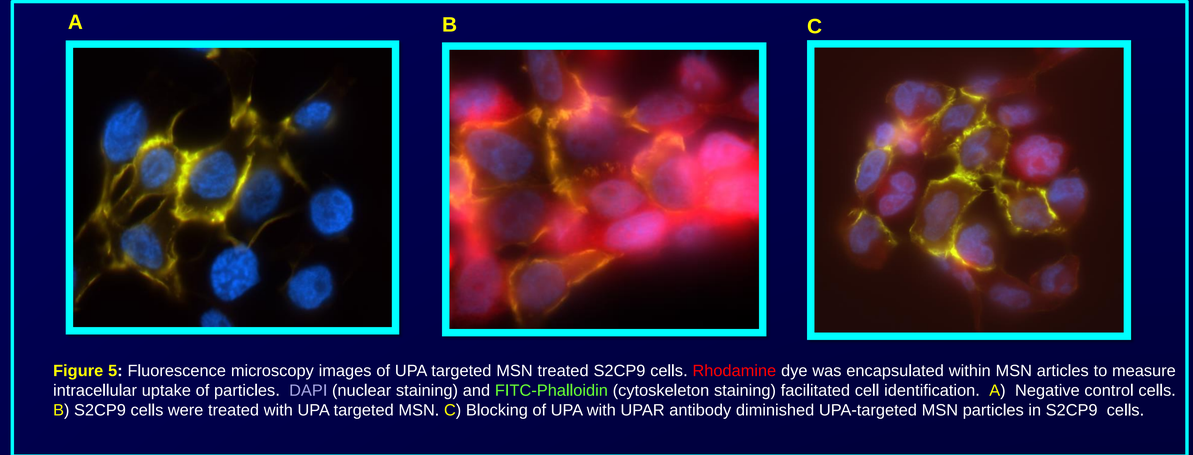

Figure 5: Fluorescence microscopy images of UPA targeted MSN treated S2CP9 cells. Rhodamine dye was encapsulated within MSN articles to measure intracellular uptake of particles. DAPI (nuclear staining) and FITC-Phalloidin (cytoskeleton staining) facilitated cell identification. A) Negative control cells. B) S2CP9 cells were treated with UPA targeted MSN. C) Blocking of UPA with UPAR antibody diminished UPA-targeted MSN particles in S2CP9 cells.

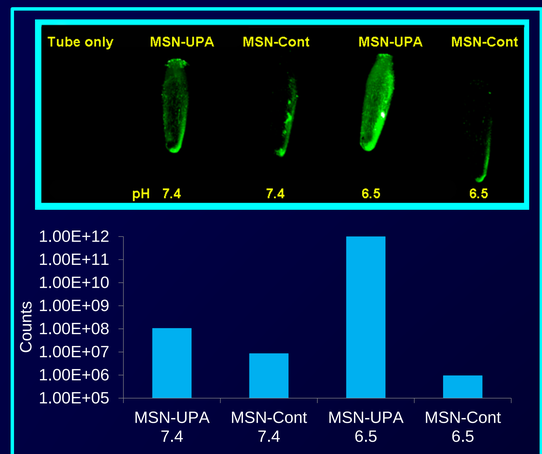

Figure 6 : Evaluation of acidic pH specificity of ICG dye release from MSNs. S2CP9 cells grown at either pH 7.4 or 6.5 were treated with either 50 µg/mL of UPA-targeted or no-ligand targeted MSNs encapsulated with ICG for 2 hours. Cells were washed with PBS and transferred into 1.5 ml tubes. Cells were viewed using Odyssey infrared imaging system with dosimetry evaluation.

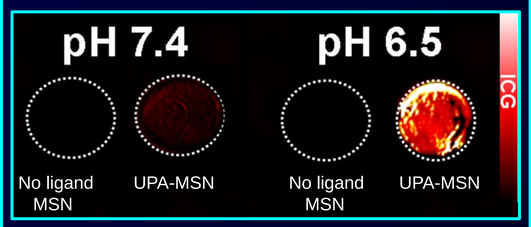

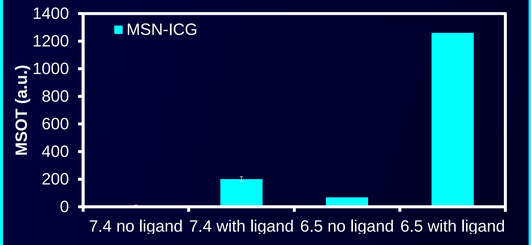

Figure 7: Visualization of targeted MSN binding to UPAR positive cells using phantoms with MSOT Cells incubated with 50 µg/mL MSN for 2 hours. Cells were washed and inserted into tissue phantoms (light scattering agar + lipid) and inserted into the MSOT.

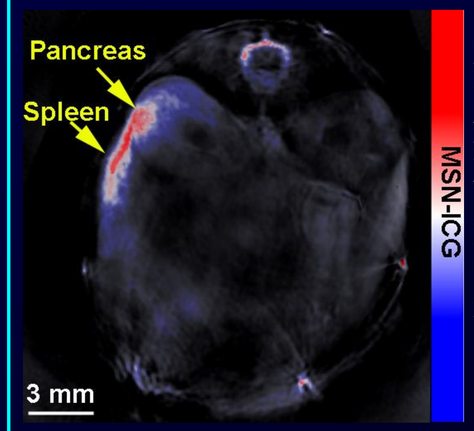

Figure 8: UPA targeted MSNs encapsulated with ICG accumulated within the pancreas tumor and spleen. The nanoparticles were injected at 1 µM by i.v. Particle accumulation was evaluated after 4 h post injection using Multispectral Optoacoustic Tomography.

CONCLUSION

- Theranostic nanoparticles offer the benefit of facilitating both tumor detection as well as containing therapeutic agents
- One of the few universal characteristics of cancer is acidic extracellular tumor microenvironment making pH sensitive therapy agents ideal
- This study illustrates the successful synthesis of pH sensitive, silica based nanoparticles (MSNs) with UPA targeting ligand for theranostic imaging of pancreatic cancer
- UPA tagged MSNs bind more effectively *in-vitro* and *in-vivo* compared to non-UPA tagged MSNs against multiple cell lines
- With further analysis and implementation of this technology, there is potential to revolutionize the detection and treatment of pancreatic cancer and other metastatic disease
- Future studies involve assessment of Gemzar release *in-vivo* and further evaluation of the MSNs using additional mice models.

ACKNOWLEDGEMENTS

This work was supported by NCI Grant CA139050 and NIH/NCI GRANT R25 - CA134283